coatings

Article

Application-Oriented Comparative Screening of SiO_2, DLC, and Raydent-Labeled Commercial Coating for High-Precision LM Guide Rails

Seung Gyeong Jeon [1,*] and Dae Yong Jeong [2]

[1] Research Institute, L-tronix Co., Ltd., Incheon 22853, Republic of Korea
[2] Department of Materials Science and Engineering, Inha University, Incheon 22212, Republic of Korea

Highlights

What are the main findings?

- SiO_2 formed the thinnest coating layer (1.03 μm), preserving LM-guide geometry.
- SiO_2 exhibited the highest composite surface hardness (719.8 HV).
- SiO_2 showed the lowest roughness and most uniform surface morphology.
- Plasma pretreatment increased hardness (580 → 720 HV) and Si signal.

What are the implications of the main findings?

- SiO_2 is a promising coating for high-precision LM-guide systems.
- Thin and smooth coatings may improve rolling-contact stability.
- Plasma-assisted interface engineering enhanced coating effectiveness.
- Further durability and adhesion tests are needed for validation.

Abstract

This study comparatively evaluated Raydent (here interpreted as a standard black chrome-type industrial condition in the present specimen context), DLC, and SiO_2 coatings for high-precision LM-guide applications as an application-oriented initial screening study. The emphasis was placed on dimensional preservation, surface integrity, and mechanical surface response rather than on complete coating-mechanism validation. Cross-sectional FE-SEM, EDS, Vickers hardness testing, surface profilometry, AFM, and SEM analyses were conducted to compare coating thickness, composite surface hardness, roughness, and morphology, and the influence of plasma pretreatment on the SiO_2 system was additionally investigated. Among the investigated coatings, SiO_2 exhibited the smallest thickness (1.03 μm), highest composite surface hardness (719.8 HV), and lowest average roughness (213.5 nm), suggesting favorable dimensional compatibility and surface integrity under the tested conditions. Plasma pretreatment increased the EDS-detected Si signal from 0.77 to 2.81 wt% and improved the composite surface hardness from 580 to 720 HV, suggesting an altered near-surface response and improvement in coating formation during pretreatment-assisted processing. AFM and SEM observations further indicated that the SiO_2 coating provided a more uniform and flatter surface morphology on the coupon specimens, whereas the DLC specimen prepared under the present commercial condition showed localized protrusions that may be associated with initial local contact disturbance. The comparative results suggest that SiO_2 coatings provide a favorable balance of thickness control, surface uniformity, composite surface hardness, and roughness for precision LM-guide applications. Although additional rolling-contact durability, adhesion, wear, friction-coefficient, and rolling-contact-fatigue studies are still required, the present findings should be interpreted as an initial screening result indicating that SiO_2 is a candidate coating condition for

Received: 17 May 2026
Revised: 19 June 2026
Accepted: 22 June 2026
Published: 24 June 2026

further engineering consideration in precision motion-guide systems, rather than as a direct validation of full tribological or long-term durability performance.

Keywords: LM guide; SiO_2 coating; DLC coating; Raydent; black chrome-type coating; AFM; SEM; surface roughness; surface morphology

1. Introduction

LM guides are core precision-motion components in semiconductor, display, machine-tool, and automation systems, where positional accuracy, repeatability, and long-term running stability depend strongly on rail geometry, contact stiffness, and rolling-surface condition [1–8].

Because these components operate under repeated rolling contact, a useful surface treatment must improve wear resistance and contact stability without introducing dimensional distortion or excessive residual stress [8,9]. From a design standpoint, coating selection therefore requires simultaneous consideration of thickness control, surface integrity, interfacial stability, and tribological behavior rather than hardness alone [10,11].

Existing surface treatments each offer only partial advantages. Commercial corrosion-protective treatments used in linear rail systems can improve environmental durability, but precision-rail applications still require careful control of coating thickness and dimensional alteration because wear- and stiffness-related performance is highly sensitive to the guideway contact condition [6–8]. DLC coatings are attractive because of their high hardness and low friction [1–4,12,13]. However, their practical use in precision components is often constrained by deposition-dependent residual stress, interfacial mismatch, temperature sensitivity, and processing cost [2–5,9,14]. TiN-based hard coatings also provide wear resistance, but their higher thickness and less favorable low-friction characteristics limit their suitability for precision rolling interfaces [15].

SiO_2 sol–gel coatings are of particular interest because they can be formed as comparatively uniform coatings at low process temperature [16,17]. Previous studies have also reported promising mechanical, corrosion-protection, and surface-stability characteristics in SiO_2-based systems [18–20]. In addition, recent work on temperature-dependent silica behavior and silica-based hybrid reinforcement suggests that coating density and composition can strongly influence mechanical performance [21,22]. Previous studies mainly focused on isolated coating properties such as hardness, friction, or corrosion resistance, whereas comparative coating-substrate evaluations considering dimensional preservation and morphology in precision LM-guide systems remain limited. Nevertheless, LM-guide applications require an integrated assessment of coating thickness, composite surface hardness, roughness, morphology, and pretreatment effects under a common component context [17,21,23]. Therefore, this study comparatively evaluates a commercial Raydent-treated surface, DLC, and SiO_2 coatings for LM-guide rails as an application-oriented screening step within a broader ongoing investigation of LM-guide mechanical behavior, while interface-related changes and their implications for guide stiffness and service life are being pursued in separate ongoing work.

2. Materials and Methods

2.1. Specimens and Coating Candidates

Commercial SUJ2-based LM-guide rail specimens were used as the substrate material, and the rails were sectioned into coupons suitable for cross-sectional microscopy, hardness testing, and surface roughness evaluation. Four surface conditions were comparatively

https://doi.org/10.3390/coatings16070747

examined: uncoated substrate, Raydent-treated surface (interpreted here as a standard black chrome-type industrial condition), DLC-coated surface, and SiO_2-coated surface. The comparison was designed to evaluate coating suitability from the viewpoint of actual LM-guide application rather than from a single-property ranking alone. Accordingly, the key assessment criteria were coating thickness, surface chemical indication by EDS, composite surface hardness, roughness, and morphology, all of which are directly related to dimensional accuracy, wear resistance, and contact stability in rolling-motion components.

2.2. Coating Preparation

For the SiO_2-coated specimens, a silica dip-coating precursor was prepared within the formulation window used in the associated coating-development process. The present SiO_2 coating belonged to a TEOS/TMOS-based mixed alkoxide precursor family within a silica-forming sol–gel formulation. The precursor consisted primarily of TEOS/TMOS (35–45 wt%) as the silica network former, an alcohol solvent (48–56 wt%), deionized water (5–9 wt%), catalyst (1–2 wt%), surfactant (0.3–0.7 wt%), silica nanoparticles (1–5 wt%), and a solid lubricant (0.1–1 wt%). No separately identified organically modified alkoxysilane such as MTMS or GPTMS was intentionally introduced in the present formulation. A representative formulation used in the present comparative study was approximately TEOS/TMOS 39 wt%, alcohol solvent 52 wt%, deionized water 6 wt%, catalyst 1 wt%, surfactant 0.5 wt%, silica nanoparticles 1 wt%, and solid lubricant 0.5 wt%. Within such a formulation, the added silica nanoparticles may have contributed to local reinforcement, stress redistribution during drying and thermal stabilization, and suppression of micro-defect formation; however, this possible role was not independently verified in the present study.

Prior to coating, the LM-guide specimens were sequentially cleaned with acetone, diluted HCl, deionized water, and warm-air drying. Dip coating was carried out at a withdrawal speed of approximately 1.5 mm s^{-1}. After dip coating, the specimens were dried at 100 °C for 30 min and then heated in an automatic laboratory furnace under continuous heating until 220 °C was reached, followed by holding at 220 °C for 1 h and furnace shutoff. Because the actual heating time depended on furnace characteristics and specimen loading, a single independently fixed ramp-rate value was not treated as a controlled variable in the present comparative study. No independent post-thermal bulk-hardness verification of the substrate was performed in the present study.

DLC-coated specimens were prepared by a commercial plasma-enhanced chemical vapor deposition (PECVD) process [1,12]. Although the detailed chamber recipe was not available, the coating was deposited under reduced-pressure industrial conditions using a hydrocarbon-based precursor system suitable for hard, low-friction carbon films on precision steel components. Because the DLC coating was treated as a commercially supplied industrial coating, the present study compares application-level coating outcomes rather than process-parameter-optimized materials. More specifically, the DLC condition investigated in this study corresponds to a supplier-side commercial S-DLC condition rather than to a fully optimized low-thickness DLC architecture designed exclusively for this research question [1,3,12].

Raydent-treated specimens were obtained using a commercial treatment route applied to LM-guide components. In the present specimen context, the Raydent designation is interpreted as a commercially used generic name in Korea corresponding to a standard black chrome-type industrial condition [24]. Because the detailed bath chemistry, reaction conditions, and process sequence are proprietary to the supplier, the exact processing parameters are not disclosed here. Because Raydent and DLC were treated as commercially supplied industrial coatings, this study compares application-level coating outcomes rather than process-parameter-optimized materials. The present comparison therefore focuses on the final coating characteristics relevant to LM-guide application, including thickness, composite surface hardness, roughness, and surface morphology.

2.3. Characterization

Cross-sectional coating thickness was examined using field-emission scanning electron microscopy (FE-SEM; Mitutoyo/Hitachi, Kanagawa, Japan) at an accelerating voltage of 10 kV and a working distance of approximately 8 mm. For each coating condition, LM-guide rail specimens were cut to an appropriate size, and their cross-sections were observed to compare the thickness of the deposited layer. Thickness values were measured at five locations from each of three specimens, and the reported values represent mean ± standard deviation. Elemental characterization was conducted using energy-dispersive X-ray spectroscopy (EDS; JSM-7600F, JEOL, Tokyo, Japan). Representative locations were selected from each coated surface, and the major elemental composition was evaluated in a qualitative or semi-quantitative manner to confirm the presence and relative enrichment of coating-related species.

Composite surface hardness measurements were carried out using a Vickers hardness tester (VHM-200, Mitutoyo, Kanagawa, Japan) under a load of 25 gf with a dwell time of 10 s. Five specimens were prepared for each surface condition, three indentations were made on each specimen, and the reported value represents mean ± standard deviation ($n = 15$) for this comparative screening study. The indentation load was selected to minimize excessive substrate influence while maintaining measurable indentation geometry. Surface roughness was measured using a surface profiler (Dektak XT, Bruker, Hamburg, Germany) over an evaluation length of 500 μm at a scan speed of 50 μm s^{-1} using a stylus tip radius of 2 μm and a cutoff length of 0.08 mm. Three specimens were examined for each surface condition, and both the maximum roughness and the average roughness were calculated. The stylus-profilometry results were used as the primary quantitative roughness metric in the present study.

For in-depth analysis of the origin of the roughness difference, additional AFM and SEM observations were carried out on super-finished substrates coated with DLC or SiO_2. AFM imaging was performed in tapping mode over a scan area of 10 μm × 10 μm using a silicon tip with a nominal radius below 10 nm, and surface SEM images were acquired at an accelerating voltage of 5 kV with a working distance of approximately 8 mm. These images were used to compare local peak formation, surface uniformity, and qualitative flatness between the two coatings. AFM images were interpreted primarily in a qualitative manner in the present study. Additional AFM roughness parameters were used for controlled local comparison, whereas the primary roughness evaluation was based on the stylus-profilometry data. This experimental design enabled a direct comparison of dimensional suitability, mechanical surface integrity, and morphology among the candidate coatings.

2.4. Plasma Surface Modification for SiO_2 Coating

To investigate whether the surface performance of the SiO_2 coating could be further improved, an additional plasma surface modification pretreatment was applied prior to SiO_2 coating using an Ar/O_2 mixed plasma (80/20 vol%) at RF power 150 W, pressure 50 Pa, for 300 s under 0.25 Torr. Two SiO_2-coated conditions were therefore compared: plasma-modified and unmodified. After coating, both conditions were analyzed by EDS and composite surface hardness testing. The comparative dataset obtained in this study suggests that the pretreatment had a beneficial influence on the coated surface response; however, the detailed optimization of plasma power, treatment time, and gas composition remains outside the scope of the present comparative screening study and should be reported in a dedicated process-optimization paper.

The present study was designed as an application-oriented screening comparison using commercially relevant LM-guide specimens. Therefore, the results should be interpreted as comparative coating–substrate system responses rather than intrinsic material properties of isolated coating films.

3. Results

3.1. Coating Thickness and Dimensional Suitability

The cross-sectional FE-SEM observations showed clear differences in mean coating thickness among the candidate surface treatments. Raydent showed the largest mean coating thickness at 13.2 µm, followed by DLC at 7.1 µm, whereas SiO_2 showed a markedly smaller mean thickness of 1.03 µm. Representative cross-sectional FE-SEM micrographs are arranged in Figure 1, and the mean measured thickness values are summarized in Table 1. For LM guides, whose operating clearance and contact geometry are controlled at the micrometer scale, this difference is not merely geometric but functionally important.

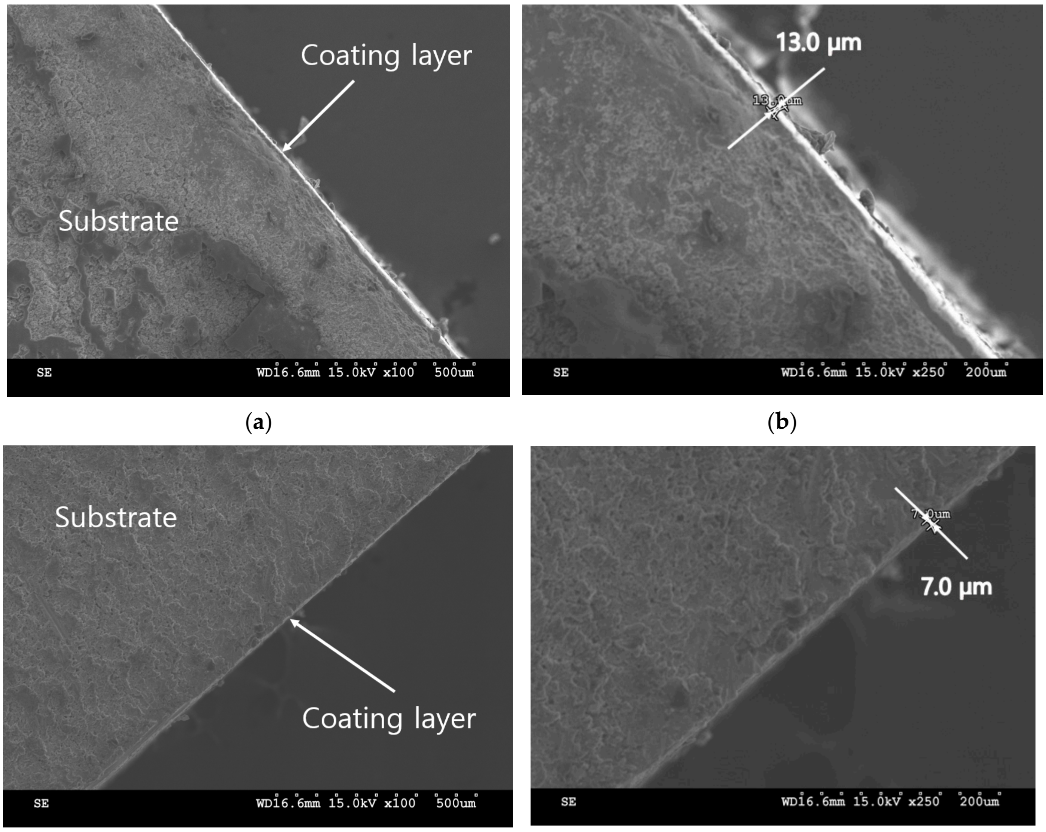

(c) (d)

Figure 1. *Cont.*

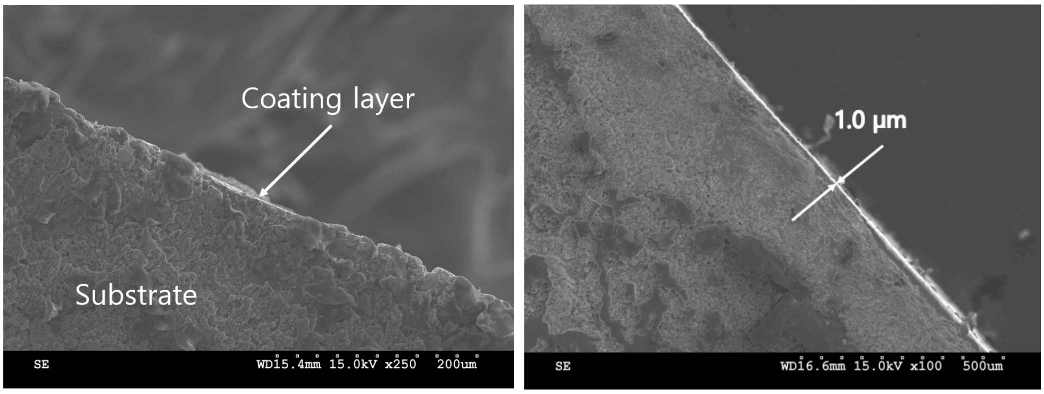

(**e**) (**f**)

Figure 1. Cross-sectional FE-SEM micrographs of the coating layers, arranged left to right as (**a**,**b**) Raydent (standard black chrome-type condition in the present specimen context) coating layer with scale bars of 500 and 200 µm, (**c**,**d**) DLC coating layer with scale bars of 500 and 200 µm, and (**e**,**f**) SiO_2 coating layer with scale bars of 500 and 200 µm.

Table 1. Mean measured coating thicknesses (mean ± SD; *n* = 15 local thickness measurements from 3 specimens) of Raydent (standard black chrome-type condition in the present specimen context), DLC, and SiO_2.

No.	Surface Treatment	Thickness (µm, Mean ± SD)
1	Raydent	13.2 ± 0.9
2	DLC	7.1 ± 0.6
3	SiO_2	1.03 ± 0.12

An excessively thick surface layer can alter the effective rail profile, disturb conformity between the raceway and rolling elements, and accumulate dimensional error during assembly. Such geometric perturbation is particularly problematic in high-precision motion systems because even a small departure from the designed contact condition can increase frictional fluctuation, degrade repeatability, and accelerate uneven stress concentration during reciprocating motion. From this viewpoint, the 1.03 µm SiO_2 layer is more favorable under the tested conditions because it provides surface modification while imposing only a minimal dimensional penalty on the rail. The result also suggests that coating suitability for LM guides should not be judged solely by the presence of a deposited layer, but by whether the coating can preserve the original mechanical geometry of the precision component. Raydent and DLC may still provide useful surface protection; however, their greater thicknesses imply a larger risk of interfering with clearance-sensitive operation unless thickness control is very tightly managed. In contrast, the much thinner SiO_2 layer is more compatible with the dimensional preservation required for precision guide applications as an initial screening result, although the practical benefit of such a thin coating must ultimately be interpreted together with its mechanical robustness and durability.

3.2. Hardness Comparison

The hardness results further distinguished the coating candidates. The average composite surface hardness of the uncoated substrate was 329.6 HV, while Raydent and DLC increased the value to 405.8 HV and 480.5 HV, respectively. The SiO_2-coated specimen exhibited the highest measured composite surface hardness, reaching 719.8 HV. A graphical comparison of the hardness values is presented in Figure 2, and the numerical values are listed in Table 2. When interpreted in relation to rolling-contact service, this ranking is meaningful because composite surface hardness is relevant to resistance against local plastic deformation, wear progression, and contact-fatigue damage at the rail-ball interface.

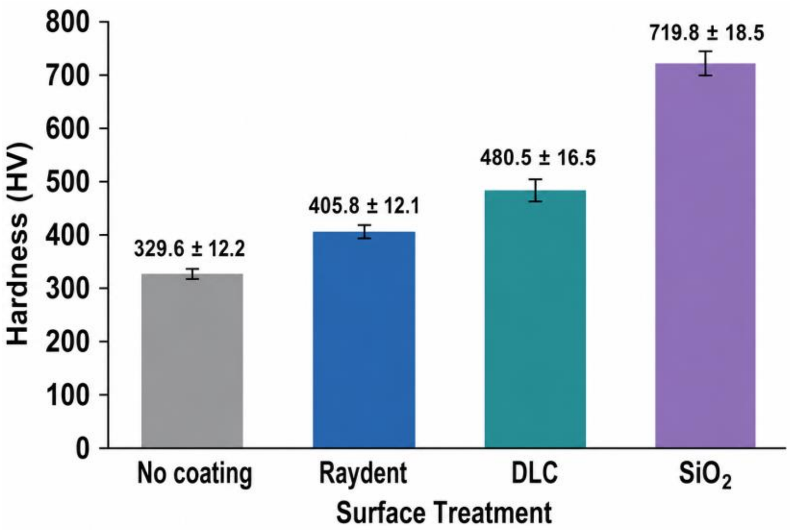

Figure 2. Comparison of mean composite surface hardness for different coating conditions (error bars indicate standard deviation).

Table 2. Mean composite surface hardness values (mean ± SD; *n* = 15 indentations from 5 specimens of the uncoated substrate, Raydent (standard black chrome-type condition in the present specimen context), DLC, and SiO_2.

No.	Surface Treatment	Composite Surface Hardness (HV)
1	No Coating	329.6 ± 12.2
2	Raydent	405.8 ± 12.1
3	DLC	480.5 ± 16.5
4	SiO_2	719.8 ± 18.5

Although hardness alone cannot fully represent rolling-contact durability, it provides a useful first-order indicator of resistance against contact-induced deformation.

Based on a previous engineering stress analysis for a comparable LM-guide ball-rail contact configuration under the rated-load condition [25], the maximum contact- rated equivalent stress was on the order of 1260 MPa. Using the Tabor hardness-yield relationship ($H \approx 3\sigma y$) [23], and assuming a yield-strength range estimated from contact stress evolution, this stress level corresponds to a critical hardness range of roughly 340–416 HV for stable resistance to contact-induced deformation. From this perspective, the uncoated substrate is close to or slightly below the desirable threshold, Raydent provides only a limited margin, and both DLC and SiO_2 exceed the critical range more convincingly. Therefore, the hardness data do not simply indicate that SiO_2 is the hardest coating; rather, they suggest that the SiO_2 and DLC coating-substrate systems may offer more favorable resistance to deformation-related damage under repeated rolling contact. This estimation is intended only as a comparative engineering guideline rather than a direct durability prediction model.

It is also important to note that the measured values should be interpreted as composite surface hardness rather than as the intrinsic hardness of the coating film alone. Because the coatings are relatively thin and supported by a steel substrate, the indentation response reflects the combined effects of coating density, interfacial integrity, surface condition, and substrate support. The particularly high value of the SiO_2-coated specimen may thus reflect the combined response of coating morphology, near-surface condition, and substrate support under the present test condition, rather than the intrinsic hardness of a 1.03 μm silica film.

The more favorable response of SiO_2 is consistent with the strong Si-O bonding network and the formation of a relatively uniform and compact coating layer, and related studies have likewise shown that the structure and mechanical response of silica-based coatings are sensitive to density, composition, and thermal history [21,22]. A relatively dense and uniform silica layer may contribute to a more stable near-surface mechanical response under the present indentation condition, thereby increasing the apparent composite resistance to indentation. By contrast, although DLC is widely known for high intrinsic hardness, the practical response of DLC coatings depends strongly on deposition conditions, the sp2/sp3 bonding ratio, residual stress, surface roughness, and interfacial state [12,14]. Accordingly, the lower hardness measured for the DLC specimen prepared under the present commercial condition should be interpreted not as a contradiction of the literature on DLC itself, but as evidence that the actual coating-substrate system produced here was less effective than the SiO_2 system in generating a high composite surface hardness.

From an application perspective, the combination of very small thickness and high composite surface hardness is of particular interest. A coating that is both dimensionally unobtrusive and mechanically robust is more desirable for precision LM guides than a thicker layer that improves hardness at the expense of assembly tolerance or contact stability. In this regard, SiO_2 showed a favorable balance among the evaluated surface conditions as an initial screening result.

3.3. Effect of Plasma Surface Modification on SiO_2 Coating

The additional plasma pretreatment was associated with a notable improvement in the SiO_2-coated specimens. The EDS-detected Si signal increased from 0.77 wt% in the unmodified condition to 2.81 wt% in the modified condition, and the average composite surface hardness increased from 580 HV to 720 HV after plasma surface modification. Because of the shallow thickness of the SiO_2 layer, the EDS results should be interpreted primarily in a qualitative or semi-quantitative sense rather than as fully quantitative compositional values. Detailed surface morphologies, EDS spectra, and element maps of the plasma-treated and untreated surfaces are presented in Figures 3 and 4; their elemental compositions are summarized in Tables 3 and 4, and the summarized EDS-detected Si-signal and hardness comparison is listed in Table 5.

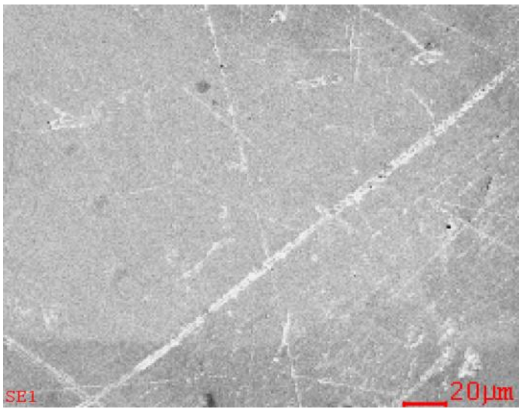

(**a**)

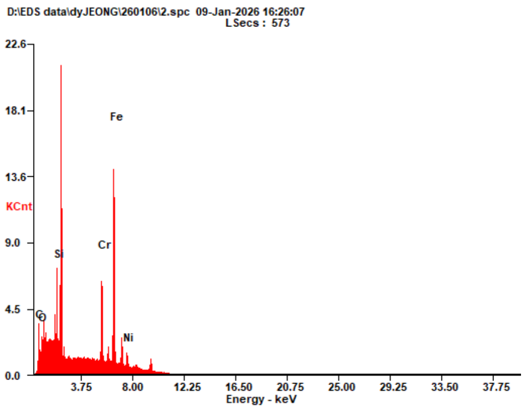

(**b**)

Figure 3. *Cont.*

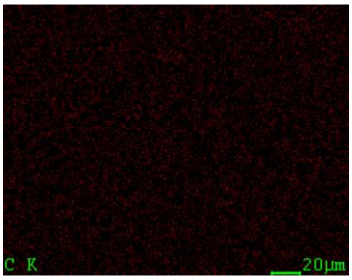

(**c**)

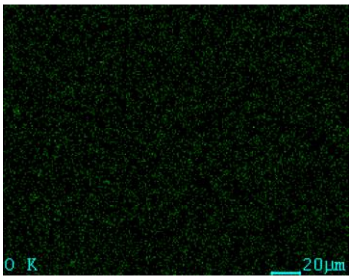

(**d**)

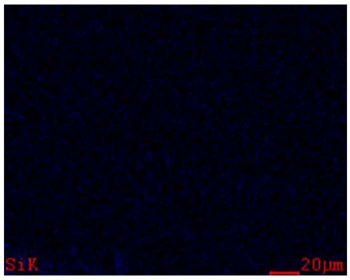

(**e**)

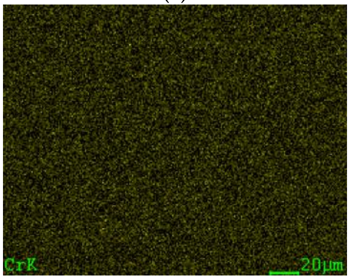

(**f**)

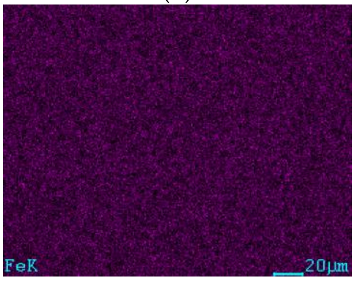

(**g**)

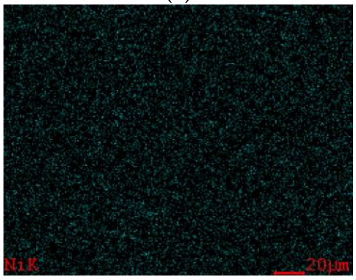

(**h**)

Figure 3. SEM image, EDS spectrum, and element maps of the plasma-treated SiO_2-coated specimen: (**a**) SEM image; (**b**) EDS spectrum; (**c**–**h**) elemental maps.

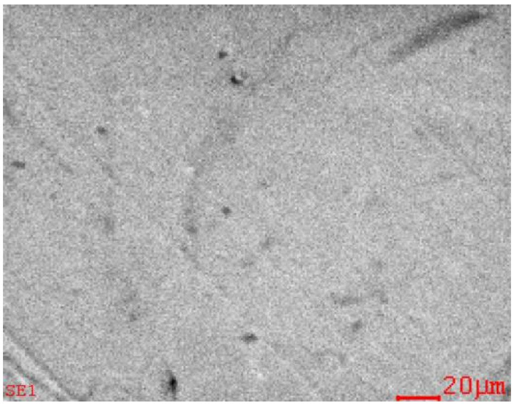

(**a**)

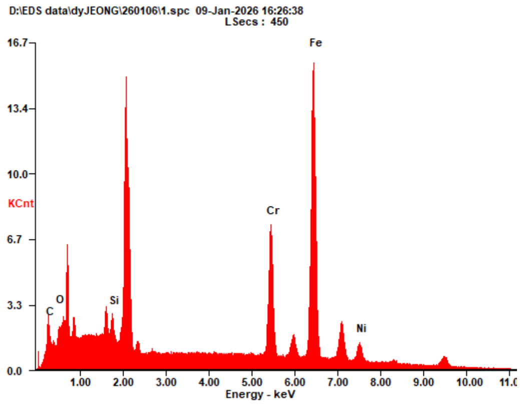

(**b**)

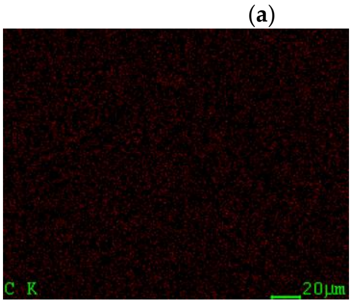

(**c**)

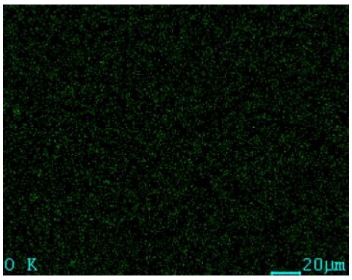

(**d**)

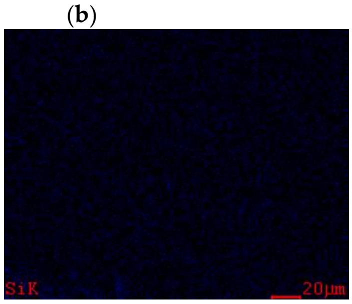

(**e**)

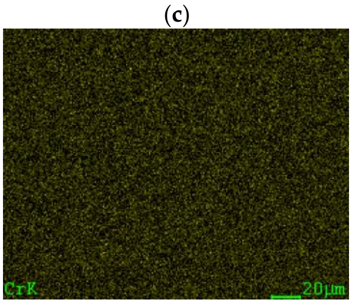

(**f**)

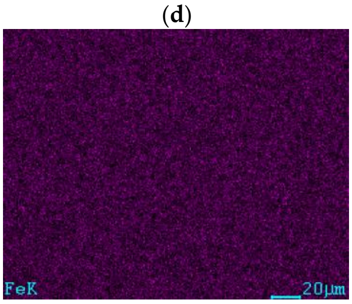

(**g**)

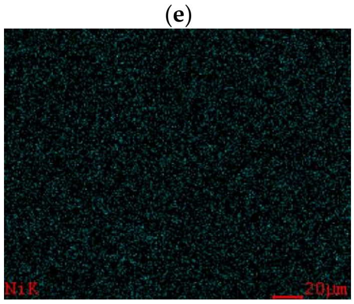

(**h**)

Figure 4. SEM image, EDS spectrum, and element maps of the untreated SiO_2-coated specimen: (**a**) SEM image; (**b**) EDS spectrum; (**c**–**h**) elemental maps.

Table 3. Semi-quantitative EDS elemental composition of the plasma-treated SiO_2-coated specimen.

Element (Plasma-Treated Specimen)	wt%	at%
CK	3.00	11.97
OK	0.75	2.23
SiK	2.81	4.79
CrK	16.50	15.22
FeK	69.06	59.33
NiK	7.89	6.45
Matrix	Correction	ZAF

Note: EDS values are semi-quantitative and represent a representative analyzed area. Because of the shallow thickness of the SiO_2 coating, the detected elemental composition should not be interpreted as a fully quantitative bulk composition.

Table 4. Semi-quantitative EDS elemental composition of the untreated SiO_2-coated specimen.

Element (Untreated Specimen)	wt%	at%
CK	2.41	10.00
OK	0.70	2.17
SiK	0.77	1.37
CrK	16.73	46.02
FeK	71.26	63.54
NiK	8.13	6.90
Matrix	Correction	ZAF

Note: EDS values are semi-quantitative and represent a representative analyzed area. Because of the shallow thickness of the SiO_2 coating, the detected elemental composition should not be interpreted as a fully quantitative bulk composition.

Table 5. Comparison of representative EDS-detected Si signal and mean composite surface hardness (mean ± SD; n = 15 indentations) between unmodified and plasma-modified SiO_2-coated specimens.

SiO_2 Condition	Representative EDS-Detected Si Signal (wt%)	Composite Surface Hardness (Mean ± SD; n = 15)
Unmodified	0.77	580 ± 29
Plasma modified	2.81	720 ± 34

Note: The EDS-detected Si signal is a representative semi-quantitative value and should be interpreted comparatively rather than as an absolute quantitative composition.

These results suggest that the pretreatment influenced not only the nominal presence of Si-containing species on the surface but also the mechanical quality of the resulting coating-substrate system. Consistent with this interpretation, the SEM/EDS results in Figures 3 and 4 indicate that the plasma-treated specimen exhibits a relatively more uniform and coherent surface morphology together with a more pronounced Si-related EDS response than the untreated specimen. Such a trend suggests that plasma exposure may have modified the near-surface condition prior to SiO_2 deposition, which may be associated with the observed changes in EDS response and composite surface hardness.

The increase in EDS-detected Si should not, however, be overinterpreted as direct proof of coating-thickness growth alone. Rather, when considered together with the SEM/EDS results in Figures 3 and 4 and the hardness increase from 580 HV to 720 HV, it is more appropriately regarded as indirect evidence that the plasma-treated surface may have modified the near-surface response associated with the observed EDS and composite-hardness changes within the analyzed region. The improved hardness is therefore likely to reflect the combined effects of possible modification of near-surface condition, reduced structural defects such as pores or weakly bonded regions, and more efficient load transfer from the coating layer into the substrate.

From an engineering perspective, this finding is important because it indicates that the performance of thin SiO_2 coatings can be improved through interface engineering rather than only by changing the bulk chemistry of the coating solution. At the same time, the present dataset does not fully resolve the underlying mechanism. Further work using contact-angle analysis, XPS, cross-sectional TEM, nano-indentation, and scratch-type adhesion evaluation would be valuable for distinguishing the relative contributions of wettability improvement, chemical activation, microstructural densification, local thickness variation, and interfacial reliability.

3.4. Surface Roughness

Surface roughness analysis also indicated a more favorable result for SiO_2 under the tested conditions. The average roughness values were 395.6 nm for the uncoated substrate, 592.7 nm for Raydent, 404.0 nm for DLC, and 213.5 nm for SiO_2. The maximum roughness values followed the same tendency, with SiO_2 showing 269.1 nm compared with 481.3 nm for the uncoated substrate, 624.0 nm for Raydent, and 496.9 nm for DLC. The summary comparison plot is shown in Figure 5, and the numerical values are listed in Table 6.

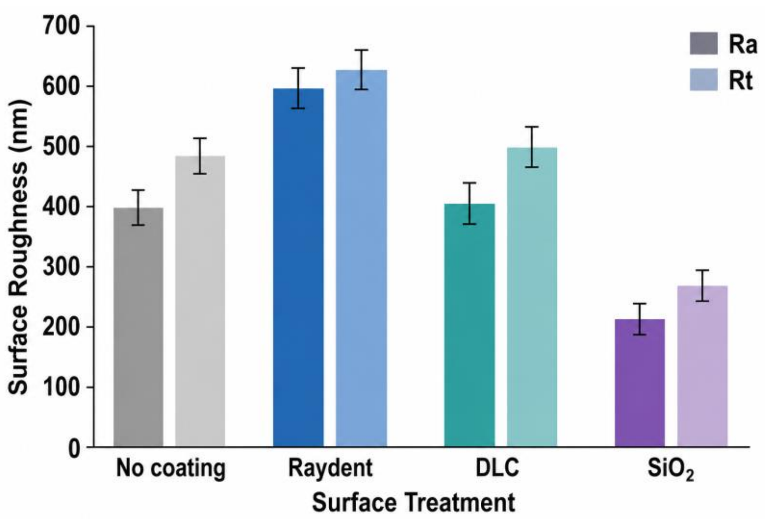

Figure 5. Comparison of mean surface roughness values for actual LM guide specimens under different coating conditions (error bars indicate standard deviation). Dark-colored bars indicate Ra values, whereas light-colored bars indicate Rt values.

Table 6. Maximum and mean roughness values on actual LM-guide specimens (mean ± SD; *n* = 3 specimens) for the compared surface conditions.

Surface Treatment	Max. Roughness (Rt, nm, Mean ± SD)	Avg. Roughness (Ra, nm, Mean ± SD)
No Coating	481.3 ± 22.6	395.6 ± 18.4
Raydent	624.0 ± 31.5	592.7 ± 27.9
DLC	496.9 ± 24.3	404.0 ± 19.6
SiO_2	269.1 ± 14.8	213.5 ± 11.9

A lower roughness value is advantageous not merely as a surface-quality indicator but as a functional parameter governing contact mechanics. A lower roughness value is advantageous not only as a surface-quality indicator but also because smoother surfaces are generally more compatible with stable initial rolling contact and reduced local geometric disturbance in precision LM-guide systems. Conversely, a smoother surface is more compatible with stable initial contact behavior.

The roughness result may also be relevant to lubrication behavior in precision rolling components, although the detailed relationship between surface morphology and lubricant-film stability was not directly investigated in the present study. The markedly lower roughness of the SiO_2-coated specimen therefore suggests a potentially more favorable balance for precision rolling components, where predictable motion and reduced contact disturbance are often more critical than aggressive texture retention.

Accordingly, the roughness data support the interpretation that SiO_2 was a more favorable candidate among the tested coating-substrate systems in terms of initial contact stability and dimensional surface integrity. Nevertheless, the ultimate tribological benefit should still be confirmed by direct rolling-fatigue and friction testing because roughness alone cannot fully represent lubricant behavior or long-term wear evolution.

3.5. Surface Morphology Comparison by AFM and SEM

To clarify the origin of the roughness difference between the SiO_2 and DLC coatings, additional surface morphology observations were performed using AFM and SEM on super-finished substrates coated with either DLC or SiO_2. It should be noted that the Ra values listed in Table 6 were measured from actual LM-guide specimens, whereas the AFM-based Ra and Rq values shown in Figure 6 were obtained from super-finished experimental substrates to enable a more controlled quantitative comparison of local surface topography. Therefore, the absolute AFM values should not be directly compared with the profilometry values of actual LM-guide specimens. The AFM images are presented in Figure 6 and the SEM images in Figure 7. Qualitatively, the DLC-coated specimen exhibited more localized protrusions and spike-like surface peaks, whereas the SiO_2-coated specimen showed a more uniform and flatter topography.

In the AFM images, the DLC surface qualitatively appeared to have larger local height variation, indicating that local asperities may have contributed to the higher roughness values measured by stylus profilometry. Additional AFM roughness parameters also supported this tendency: the SiO_2-coated surface showed Ra and Rq values of 31.336 and 49.33 nm, respectively, whereas the DLC-coated surface showed corresponding values of 41.903 and 68.999 nm. By contrast, the SiO_2-coated surface showed fewer local protrusions and a smoother topographical profile, which is consistent with the lower average roughness and with the smoother surface evolution often observed in carefully deposited sol–gel-derived silica coatings. This qualitative difference is important because isolated peaks can dominate the earliest stage of contact, even when the average surface condition appears acceptable.

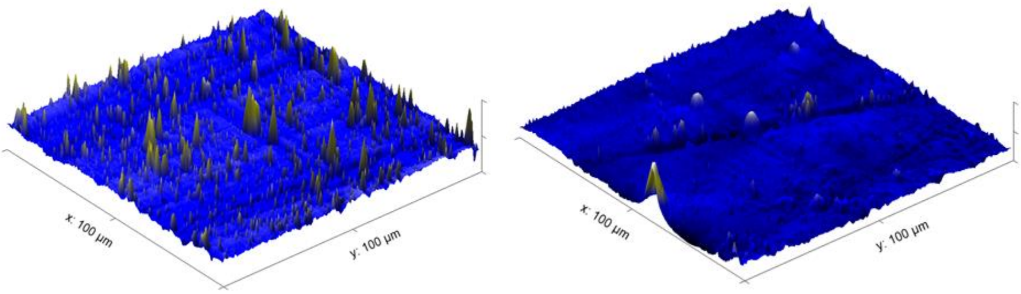

(**a**) (**b**)

Figure 6. Representative AFM images of super-finished coated substrates used for local morphology comparison: (**a**) DLC-coated specimen (Ra = 41.903 nm, Rq = 68.999 nm); (**b**) SiO_2-coated specimen (Ra = 31.336 nm, Rq = 49.33 nm). Color contrast represents relative surface-height variation in the AFM topography, where blue regions indicate lower surface areas and bright regions indicate higher asperities.

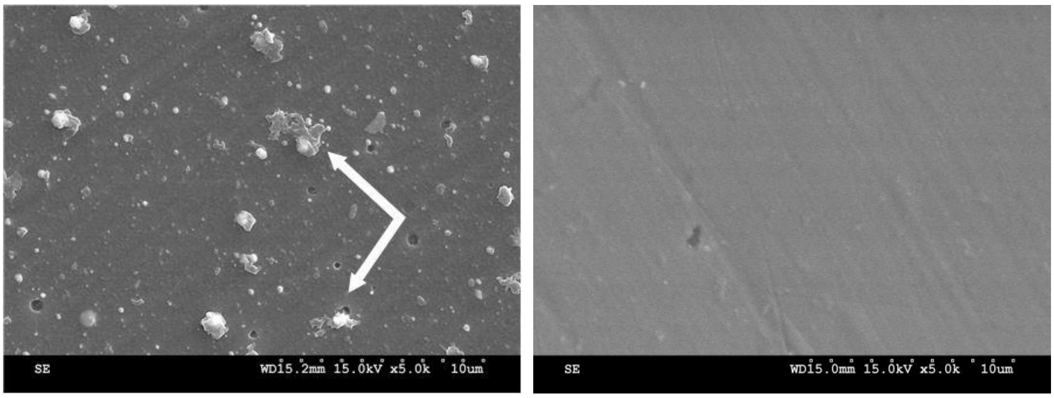

(**a**) (**b**)

Figure 7. Representative SEM images of super-finished coated substrates used for local morphology comparison: (**a**) DLC-coated specimen showing localized bright protrusions; (**b**) SiO_2-coated specimen showing a comparatively uniform surface morphology. Arrows indicate representative droplet-like surface protrusions observed on the DLC coating.

The SEM observations generally supported the AFM results. The SiO_2 coating displayed a relatively homogeneous morphology without pronounced granular boundaries or directional growth features, whereas the DLC surface contained localized bright protrusions in the representative SEM view. The correspondence between protruded features in SEM and local height excursions in AFM suggests that the roughness difference is associated with a microstructural distinction between the two coatings.

These protrusions on the DLC surface may originate from particle re-attachment during deposition, local non-uniformity of the amorphous carbon structure, or the trapping of residual particles from pretreatment or handling. Although the present data are insufficient to determine the exact origin, the practical implication is that a surface containing more isolated high peaks may be more likely to generate local contact-pressure spikes, friction fluctuation, and early run-in wear. By contrast, the flatter SiO_2 surface may contribute to a more stable initial contact state and less severe asperity-driven damage.

At the same time, this interpretation should remain balanced. A smoother SiO_2 surface does not automatically guarantee more favorable long-term durability under all operating conditions, because ceramic-like coatings may also exhibit brittle cracking or local spalling if the interface or subsurface support is insufficient. Thus, the AFM/SEM observations should be regarded as evidence consistent with better initial surface integrity for SiO_2, while the final relative performance under service conditions still requires confirmation through repeated rolling-contact tests.

4. Discussion

The present results show that coating selection for high-precision LM guides cannot be made on hardness alone. Although previous studies reported friction and wear benefits of DLC-coated bearing or LM-guide systems [26,27], the present comparison indicates that a useful coating for precision rails must simultaneously satisfy minimal dimensional intrusion, adequate resistance to contact-induced deformation, low surface roughness, and a morphology that does not destabilize initial rolling contact. Evaluating only one parameter in isolation can therefore lead to a misleading ranking of coating suitability. Previous DLC studies primarily emphasized friction reduction and wear protection [26,27], whereas the present study indicates that dimensional preservation and surface morphology are equally critical for LM-guide applications. This distinction is important because even a mechanically hard coating may become less attractive if it introduces geometric interference or unstable local contact conditions during the early stages of rolling motion. Adhesion behavior may become especially important for ceramic-like thin films because interface failure can dominate practical durability.

From this integrated perspective, Raydent was disadvantaged primarily by its relatively large thickness and high roughness, despite providing a moderate hardness increase over the uncoated condition. DLC provided a more substantial hardness improvement, but its thicker layer relative to SiO_2 and its protrusion-rich surface morphology reduced its attractiveness for precision applications where micrometer-scale form preservation and stable contact initiation are critical. In other words, the DLC specimen prepared under the present commercial conditions remained mechanically promising but geometrically and morphologically less favorable under the tested conditions. This does not mean that DLC is inherently unfavorable for LM-guide applications. Different DLC architectures, deposition conditions, and thickness designs may lead to substantially different dimensional and surface responses, and some optimized DLC conditions may achieve characteristics comparable to those observed for SiO_2 in the present study. Accordingly, the present paper should be understood as an LM-oriented screening comparison of the tested coating conditions rather than as a generalized negative judgment on DLC as a coating family.

By contrast, SiO_2 combined the thinnest coating thickness with the highest measured composite surface hardness and the lowest roughness, while the AFM/SEM observations further suggested a more uniform and flatter surface. This multi-criteria advantage is important because LM-guide performance depends simultaneously on assembly tolerance, contact stability, frictional behavior, and long-term wear resistance. The present study is therefore consistent with the view that the favorable response of SiO_2 does not arise from a single exceptional property, but from a favorable balance among several functionally coupled properties observed in this initial screening.

The plasma pretreatment result further suggests that the performance of SiO_2 coatings may be improved through interface engineering as well as through coating chemistry. The increase in EDS-detected Si signal and composite surface hardness after pretreatment is consistent with a scenario in which surface activation may improve the near-surface response associated with coating formation and interfacial load transfer. This implies that optimization of pretreatment conditions may be an effective route for further improving coating performance without sacrificing the thickness advantage that makes SiO_2 attractive for precision LM guides.

For precision semiconductor and display transport systems, where micrometer-scale assembly tolerance and contact stability are critical, coating dimensional compatibility may become as important as hardness or wear resistance. In such applications, the practical value of a coating is determined not only by its protective function but also by whether it preserves the designed guide geometry and stable rolling contact under service conditions.

The present study does not provide full chemistry–structure characterization of the coating systems, particularly with respect to the bonding structure and spectroscopic features of the DLC layer, and this remains an important limitation of the current screening work. Low-temperature-stabilized SiO_2 coatings may also retain a certain degree of residual porosity. Under rolling-contact loading, such porosity may either help accommodate local stress and retard crack propagation or, conversely, act as a structural flaw that promotes local damage initiation; this point was not experimentally resolved in the present study.

Accordingly, the present work should be interpreted as an application-oriented comparative screening study within a broader system-level investigation of LM-guide mechanical behavior, while detailed interface-related effects and their implications for stiffness and service life are being pursued in separate ongoing work. In this context, additional work is required to quantify friction coefficient, adhesion strength, repeated rolling-contact durability, lubricant retention behavior, residual stress, and the possibility of local brittle damage of the SiO_2 layer. Future studies should also correlate AFM/SEM-observed morphology with run-in wear and contact-stress evolution.

5. Conclusions

The major findings of this study can be summarized as follows.

(1) SiO_2 formed the thinnest coating layer, with a thickness of 1.03 μm, compared with 7.1 μm for DLC and 13.2 μm for Raydent. Under the present comparative conditions, this smaller thickness was more favorable from the standpoint of preserving rail geometry and assembly tolerance in high-precision LM-guide systems.

(2) SiO_2 exhibited the highest measured composite surface hardness of 719.8 HV, whereas the corresponding values of the uncoated substrate, Raydent, and DLC were 329.6 HV, 405.8 HV, and 480.5 HV, respectively. This indicates that SiO_2 showed a favorable composite surface hardness response among the tested coating-substrate systems.

(3) SiO_2 showed the lowest average surface roughness of 213.5 nm, outperforming the uncoated substrate, DLC, and Raydent conditions. This smoother surface may potentially contribute to reduced asperity-driven stress concentration during the early stage of rolling contact.

(4) Plasma surface modification improved the composite surface hardness of the SiO_2-coated surface from 580 HV to 720 HV and increased the EDS-detected Si signal from 0.77 wt% to 2.81 wt%, indicating that pretreatment-assisted interface control may enhance coating effectiveness.

(5) AFM and SEM observations on the coupon specimens suggested that the SiO_2 coating had a more uniform and flatter surface, whereas the DLC coating exhibited localized protrusions and spike-like peaks that may increase local contact instability during early-stage rolling contact.

Overall, among the compared surface conditions, SiO_2 exhibited a favorable combination of dimensional preservation, surface integrity, and mechanical response under the investigated experimental conditions. Nevertheless, the present findings should be interpreted as an initial screening result indicating that SiO_2 is a candidate condition for further engineering consideration, and not as a direct validation of full tribological or long-term durability performance. Its practical suitability should therefore be validated further through direct repeated rolling-contact and long-term durability testing, particularly with respect to adhesion reliability, brittle damage, thermal-exposure effects, and lubricant-assisted service behavior.

6. Patents

A patent application related to this work has been filed in the Republic of Korea under application number 10-2025-0135273, entitled "Coating Method for Linear Guide Rail and Linear Guide Rail Manufactured Thereby".

Author Contributions: Conceptualization, S.G.J. and D.Y.J.; methodology, S.G.J.; validation, S.G.J.; formal analysis, S.G.J.; investigation, S.G.J.; data curation, S.G.J.; writing—original draft preparation, S.G.J.; writing—review and editing, D.Y.J.; supervision, D.Y.J. All authors have read and agreed to the published version of the manuscript.

Funding: This research was supported by the Industry-Academia Collaboration Project for SMEs funded by the Ministry of SMEs and Startups (MSS), Republic of Korea, under grant number RS-2025-02220593, "Development of an Integrated Mini Linear Robot with a Rail Width of 30 mm and a Stroke of 300 mm".

Institutional Review Board Statement: Not applicable.

Informed Consent Statement: Not applicable.

Data Availability Statement: The data presented in this study are available from the corresponding author on reasonable request.

Acknowledgments: During the preparation of this manuscript, the authors used ChatGPT (OpenAI, GPT-5.5) for English language refinement and editorial assistance. The authors reviewed and edited the output and take full responsibility for the content of this publication.

Conflicts of Interest: Author Seung Gyeong Jeon was employed by the company Research Institute, L-tronix Co., Ltd. The remaining authors declare that the research was conducted in the absence of any commercial or financial relationships that could be construed as potential conflicts of interest. The funder had no role in the design of the study; in the collection, analyses, or interpretation of data; in the writing of the manuscript; or in the decision to publish the results.

Abbreviations

The following abbreviations are used in this manuscript:

LM	Linear Motion
DLC	Diamond-Like Carbon
FE-SEM	Field-Emission Scanning Electron Microscopy
EDS	Energy-Dispersive X-ray Spectroscopy
AFM	Atomic Force Microscopy
PECVD	Plasma-Enhanced Chemical Vapor Deposition
RF	Radio Frequency
TEOS	Tetraethyl Orthosilicate
TMOS	Tetramethyl Orthosilicate
XPS	X-ray Photoelectron Spectroscopy

References

1. Khun, N.W.; Neville, A.; Kolev, I.; Zhao, H. Friction and Wear of DLC Coating Deposited on M2 Steel via μW-PECVD Against 100Cr6 Steel with Different Normal Loads and Sliding Speeds Under Dry and Lubrication Conditions. *Tribol. Ind.* **2024**, *46*, 570–588. [CrossRef]
2. Shanmugasundar, G.; Vanitha, M.; Logesh, K.; Cepova, L.; Elangovan, M. Effect of deposition temperature on the tribo-mechanical properties of nitrogen doped DLC thin film. *Front. Mech. Eng.* **2024**, *10*, 1365555. [CrossRef]
3. Shaikh, S.; Sadeghi, M.; Cruz, S.; Ferreira, F. Recent Progress on the Tribology of Pure/Doped Diamond-like Carbon Coatings and Ionic Liquids. *Coatings* **2024**, *14*, 71. [CrossRef]
4. Liu, K.; Ding, Q.; Peng, H.; Guan, K.; Xi, X.; Kong, N.; Liao, M. Tribological Properties of Multilayer DLC/MoS2 Nanocomposite Coatings on Microtextured Titanium Alloy Surfaces. *Lubricants* **2024**, *12*, 374. [CrossRef]
5. Li, H.; Liu, C.; Sun, P.; Zhang, J. Enhanced adhesion and wear resistance of DLC films on AZ31 alloy achieved with high bias voltage. *Heliyon* **2024**, *10*, e38864. [CrossRef] [PubMed]
6. Tao, W.; Zhong, Y.; Feng, H.; Wang, Y. Model for wear prediction of roller linear guides. *Wear* **2013**, *305*, 260–266. [CrossRef]
7. Zou, H.T.; Wang, B.L. Investigation of the contact stiffness variation of linear rolling guides due to the effects of friction and wear during operation. *Tribol. Int.* **2015**, *92*, 472–484. [CrossRef]
8. Kang, E.G.; Lee, D.Y.; Kim, S.Y. The performance test on Me-DLC films for improving wear resistance of LM-guide. *J. Korean Soc. Precis. Eng.* **2012**, *29*, 409–416. Available online: https://www.kci.go.kr/kciportal/ci/sereArticleSearch/ciSereArtiView.kci?sereArticleSearchBean.artiId=ART001643837 (accessed on 17 May 2026). [CrossRef]
9. Mogensen, K.S.; Pfohl, C.; Rie, K.T.; Guiberteau, E. Development of an industrialised DLC duplex treatment process. *Surf. Coat. Technol.* **2002**, *151–152*, 462–465. [CrossRef]
10. Zhang, Y.; Shakil, A.; Wang, H.; Li, X.; Tang, H.; Polycarpou, A.A. Effects of SiO_2 content on the nanomechanical properties of CoCrPt-SiO_2 granular films. *Sci. Rep.* **2019**, *9*, 17580. [CrossRef] [PubMed]
11. El-Awadi, G.A. Review of effective techniques for surface engineering material modification for a variety of applications. *AIMS Mater. Sci.* **2023**, *10*, 652–692. [CrossRef]
12. Rajak, D.K.; Kumar, A.; Behera, A.; Menezes, P.L. Diamond-Like Carbon (DLC) Coatings: Classification, Properties, and Applications. *Appl. Sci.* **2021**, *11*, 4445. [CrossRef]

13. Topolovec-Miklozic, K.; Lockwood, F.; Spikes, H. Behaviour of boundary lubricating additives on DLC coatings. *Wear* **2008**, *265*, 1893–1901. [CrossRef]
14. Zhong, W.; Wang, H.; Ma, L.; Zhang, C. Impact abrasive wear of Cr/W-DLC/DLC multilayer films at various temperatures. *Metals* **2022**, *12*, 1981. [CrossRef]
15. Gopi, R.; Saravanan, I.; Devaraju, A.; Sivasamy, P. A review on recent progress in PVD-TiN coatings. *Diffus. Found. Mater. Appl.* **2023**, *34*, 41–53. [CrossRef]
16. Galliano, P.; De Damborenea, J.J.; Pascual, M.J.; Duran, A. Sol-gel coatings on 316L steel for clinical applications. *J. Sol-Gel Sci. Technol.* **1998**, *13*, 723–727. [CrossRef]
17. Cairns, D.R.; Kessman, A.J.; Richter, P.J.; Bottari, F.J.; Randall, N.X. Mechanical and tribological investigations of sol-gel derived SiO_2 optical coatings. *Wear* **2008**, *265*, 411–416. [CrossRef]
18. Pavlovska, H.; Malnieks, K.; Mezinskis, G.; Bidermanis, L.; Karpe, M. Hard TiO_2-SiO_2 sol-gel coatings for enamel against chemical corrosion. *Surf. Coat. Technol.* **2014**, *258*, 206–210. [CrossRef]
19. Gallardo, J.; Garcia, I.; Celis, J.P.; Arenas, M.A.; Conde, A.; Duran, A. Effect of sintering temperature on the corrosion and wear behavior of protective SiO_2-based sol-gel coatings. *J. Sol-Gel Sci. Technol.* **2003**, *27*, 175–183. [CrossRef]
20. Atik, M.; de Lima Neto, P.; Avaca, L.A.; Aegerter, M.A.; Zarzycki, J. Protection of 316L stainless steel against corrosion by SiO_2 coatings. *J. Mater. Sci. Lett.* **1994**, *13*, 1081–1085. [CrossRef]
21. Vivar Mora, L.; Taylor, A.; Paul, S.; Dawson, R.; Wang, C.; Taleb, W.; Owen, J.; Neville, A.; Barker, R. Impact of silica nanoparticles on the morphology and mechanical properties of sol-gel derived coatings. *Surf. Coat. Technol.* **2018**, *342*, 48–56. [CrossRef]
22. Ballarre, J.; Jimenez-Pique, E.; Anglada, M.; Pellice, S.A.; Cavalieri, A.L. Mechanical characterization of nano-reinforced silica-based sol–gel hybrid coatings on AISI 316L stainless steel using nanoindentation techniques. *Surf. Coat. Technol.* **2009**, *203*, 3325–3331. [CrossRef]
23. Tabor, D. *The Hardness of Metals*; Clarendon Press: Oxford, UK, 1951.
24. Abdel Hamid, Z. Electrodeposition of black chromium from environmentally electrolyte based on trivalent chromium salt. *Surf. Coat. Technol.* **2009**, *203*, 3442–3449. [CrossRef]
25. Jeon, S.G.; Huh, W. Fatigue Analysis of a Linear Actuator. *Trans. Korean Soc. Mech. Eng. A* **2023**, *47*, 471–479. [CrossRef]
26. He, F.; Wong, P.L.; Zhou, X. Wear properties of DLC-coated steel rollers running with highly contaminated lubrication. *Tribol. Int.* **2010**, *43*, 990–996. [CrossRef]
27. Podgornik, B.; Jacobson, S.; Hogmark, S. DLC coating of boundary lubricated components—Advantages of coating one of the contact surfaces rather than both or none. *Tribol. Int.* **2003**, *36*, 843–849. [CrossRef]